

See discussions, stats, and author profiles for this publication at: <https://www.researchgate.net/publication/261995766>

# Visible Light-Driven Cross-Coupling Reactions at Lower Temperatures Using a Photocatalyst of Palladium and Gold Alloy Nanoparticles

ARTICLE in ACS CATALYSIS · APRIL 2014

Impact Factor: 9.31 · DOI: 10.1021/cs5000284

---

CITATIONS

10

READS

96

## 9 AUTHORS, INCLUDING:



Qi Xiao

Queensland University of Technology

14 PUBLICATIONS 148 CITATIONS

[SEE PROFILE](#)



Jianfeng Jia

Shanxi Normal University

45 PUBLICATIONS 247 CITATIONS

[SEE PROFILE](#)



Haishun Wu

27 PUBLICATIONS 232 CITATIONS

[SEE PROFILE](#)



H. Y. Zhu

Queensland University of Technology

189 PUBLICATIONS 7,408 CITATIONS

[SEE PROFILE](#)

# Visible Light-Driven Cross-Coupling Reactions at Lower Temperatures Using a Photocatalyst of Palladium and Gold Alloy Nanoparticles

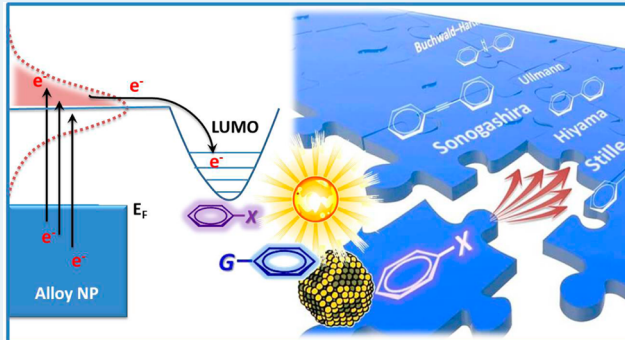
Qi Xiao,<sup>†</sup> Sarina Sarina,<sup>†</sup> Arixin Bo,<sup>†</sup> Jianfeng Jia,<sup>‡</sup> Hongwei Liu,<sup>†</sup> Dennis P. Arnold,<sup>†</sup> Yiming Huang,<sup>†</sup> Haishun Wu,<sup>‡</sup> and Huaiyong Zhu<sup>\*,†</sup>

<sup>†</sup>School of Chemistry, Physics and Mechanical Engineering, Faculty of Science and Technology, Queensland University of Technology, Brisbane, QLD 4001, Australia

<sup>‡</sup>School of Chemical and Material Science, Shanxi Normal University, Linfen 041004, China

**ABSTRACT:** Palladium (Pd)-catalyzed cross-coupling reactions are among the most important methods in organic synthesis. We report the discovery of highly efficient and green photocatalytic processes by which cross-coupling reactions, including Sonogashira, Stille, Hiyama, Ullmann, and Buchwald–Hartwig reactions, can be driven with visible light at temperatures slightly above room temperature using alloy nanoparticles of gold and Pd on zirconium oxide, thus achieving high yields. The alloy nanoparticles absorb visible light, and their conduction electrons gain energy, which is available at the surface Pd sites. Results of the density functional theory calculations indicate that transfer of the light excited electrons from the nanoparticle surface to the reactant molecules adsorbed on the nanoparticle surface activates the reactants. When the light intensity was increased, a higher reaction rate was observed, because of the increased population of photoexcited electrons. The irradiation wavelength also has an important impact on the reaction rates. Ultraviolet irradiation can drive some reactions with the chlorobenzene substrate, while visible light irradiation failed to, and substantially improve the yields of the reactions with the bromobenzene substrate. The discovery reveals the possibility of using low-energy and -density sources such as sunlight to drive chemical transformations.

**KEYWORDS:** alloy nanoparticles, cross-coupling, photocatalysis, surface plasmon resonance, visible light



## 1. INTRODUCTION

Palladium-based catalysts are widely used in cross-coupling reactions for the formation of carbon–carbon bonds. A large variety of homogeneous catalytic systems based on Pd(II) or Pd(0) have become powerful and versatile tools in modern organic synthesis,<sup>1–3</sup> being employed from the total synthesis of natural products to the preparation of new materials to bioorganic chemistry.<sup>4,5</sup> In addition, recent years have seen the imperative to develop “green” cross-coupling reactions using more environmentally friendly catalysts and methods.<sup>4</sup> For example, Pd nanoparticles (PdNPs) have emerged as promising catalysts that can function under moderate conditions and be recycled more readily,<sup>6,7</sup> although the catalytic efficiency of the NPs is often not as good as that of the homogeneous Pd catalysts. Many of the catalytic reactions (with homogeneous Pd catalysts or PdNP catalysts) are thermally driven to achieve viable efficiency, but the heating also has negative side effects. For example, it makes the synthesis reactions energy-intensive as we have to heat the entire reaction system, including the reactor and solvent. High reaction temperatures may also increase the extent of formation of unwanted side products in some reactions.<sup>8–11</sup> Furthermore, heating may compromise

catalysts’ stability and reusability. Thus, new catalytic systems based on efficient, recyclable catalysts and green energy sources for effective chemical transformations are highly desirable but remain a significant challenge.

Light is one potentially sustainable energy source with which to drive chemical reactions.<sup>12–19</sup> Very recently, we discovered that Au–Pd alloy NPs can strongly absorb visible light and efficiently enhance the extents of conversion of several reactions, including the Suzuki–Miyaura cross-coupling reactions, at temperatures slightly above room temperature.<sup>19</sup> Two other research groups also found almost at the same time that it is an effective approach to use irradiation to accelerate Suzuki cross-coupling reactions by using Au–Pd bimetallic nanostructures.<sup>20,21</sup> We believe that the conduction electrons of the NPs gain the energy of the incident light, generating electrons at high energy levels (light-excited electrons). These light-excited electrons are available at the surface Pd sites of the alloy NPs. The surface Pd sites have good affinity for the reactant

Received: January 9, 2014

Revised: April 1, 2014



molecules, and the electrons at these sites enhance their intrinsic ability to activate the reactant molecules. The charge heterogeneity of the alloy NP surface, because of the different electronegativities of gold and palladium, also plays a key role in the catalytic reactions. The proposed mechanism of light-excited electrons of alloy NPs and the interaction of the adsorbed reactant molecules with the excited electrons and the NP surface is not specific to the Suzuki–Miyaura cross-coupling reaction. It is rational to hypothesize that the Au–Pd alloy structure is likely to be efficient for driving a variety of Pd-catalyzed cross-coupling reactions with visible light. A challenge is that the activation of various reactant molecules for different reactions may not be the same, but the study of several cross-coupling reactions can provide insight into the mechanism of the photocatalytic cross-coupling processes in general.

In this study, five different cross-coupling reactions were investigated to confirm the general applicability of Au–Pd alloy NP photocatalysts under visible light irradiation, namely, the Sonogashira, Stille, Hiyama, and Ullmann C–C couplings and the Buchwald–Hartwig amination (C–N cross-coupling). We found that visible light can drive these cross-coupling reactions with the alloy NP catalyst at temperatures slightly above room temperature, and the performance of the alloy catalyst depends on the intensity and wavelength of the light irradiation. A mechanism is proposed on the basis of the results of the density functional theory (DFT) calculations and experimental observation: light absorption of the alloy NPs generates excited electrons, and the light-excited electrons with sufficient energy are able to transfer into the lowest unoccupied molecular orbital (LUMO) of the reactant molecules adsorbed on the NPs, weakening the chemical bonds of the molecules and facilitating the reactions.

## 2. RESULTS AND DISCUSSION

**2.1. Catalyst Synthesis and Characterization.** In this study, Au–Pd NPs were supported on zirconia ( $\text{ZrO}_2$ ) powder as photocatalysts (for the detailed method, see the Experimental Section). The NPs of pure gold and pure palladium on the  $\text{ZrO}_2$  support ( $\text{AuNPs@ZrO}_2$  and  $\text{PdNPs@ZrO}_2$ ) were also prepared under synthetic conditions similar to those used for the synthesis of the alloy NPs. Figure 1 shows the transmission electron microscopy (TEM) analysis of the alloy NPs; the Au–Pd alloy NPs are distributed evenly on the  $\text{ZrO}_2$  particle surface, and the mean diameters of the Au–Pd alloy NPs are  $<7$  nm (Figure 1b). The elemental composition of the as-prepared Au–Pd alloy NPs was studied using energy dispersion X-ray spectroscopy (EDX). As shown in Figure 1e, line scan analysis for a typical Au–Pd alloy NP shows that Au and Pd are distributed fairly uniformly in an alloy NP.

The important feature of the Au–Pd alloy NPs, which makes them useful in photocatalysis, is that they strongly absorb visible light mainly through the localized surface plasmon resonance (LSPR) effect of AuNPs.<sup>19–21</sup> Figure 2 shows the diffuse reflectance ultraviolet–visible extinction (DR UV-vis) spectra of the samples. Here, the spectrum of the Au–Pd alloy NP sample is clearly different from the spectra of the pure metal NPs. The  $\text{ZrO}_2$  support exhibited little absorption of light with wavelengths longer than 400 nm. Hence, the light absorption in the spectra of the Au–Pd alloy  $\text{NPs@ZrO}_2$  samples, which is the difference between light absorption of the  $\text{NPs@ZrO}_2$  and that of the  $\text{ZrO}_2$  support alone, is due to the absorption of the alloy NPs.<sup>22,23</sup> The difference between the two spectra of supported and colloid metal NPs can be

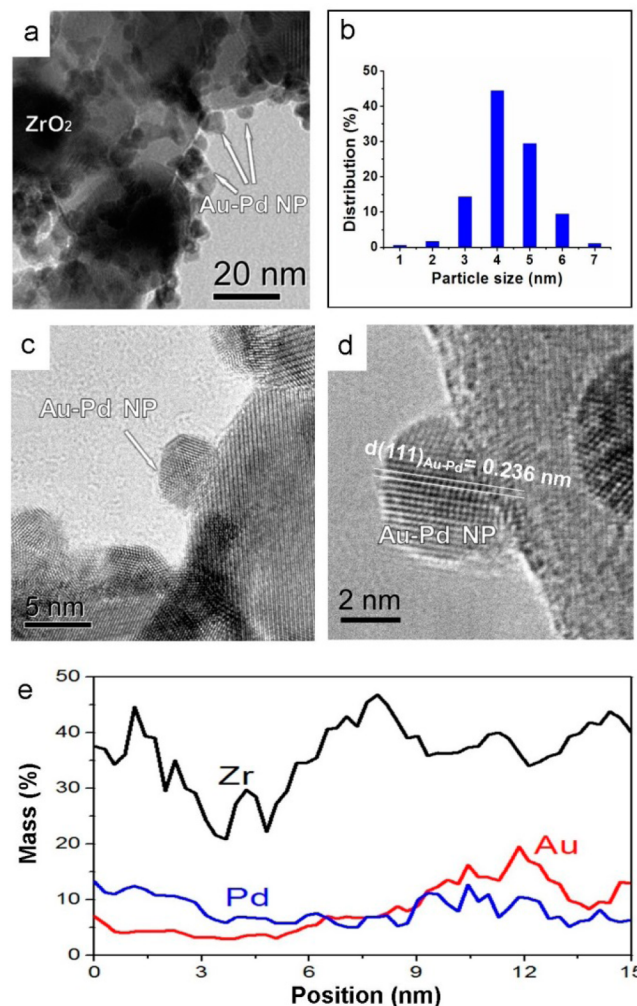


**Figure 1.** (a) TEM image of the Au–Pd alloy NPs. (b) Particle size distribution of the Au–Pd alloy NPs. (c and d) High-resolution TEM (HR-TEM) images of the Au–Pd alloy NPs. (e) Line profile analysis of a typical Au–Pd NP providing information about the elemental composition and Au/Pd distribution of the NP.

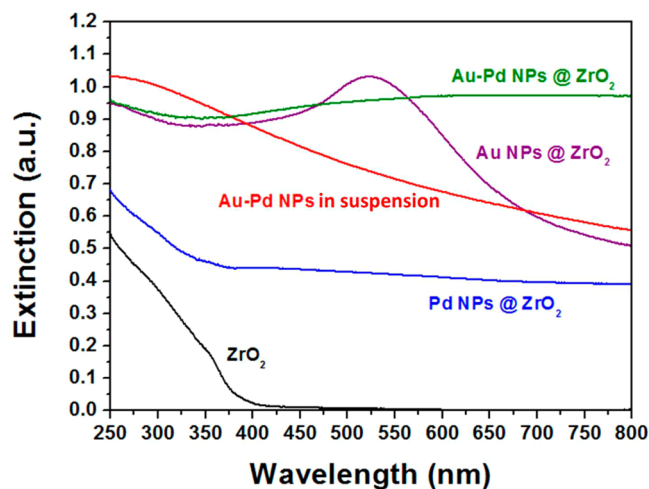


**Figure 2.** DR UV-vis spectra of the Au–Pd alloy  $\text{NPs@ZrO}_2$  catalyst and their comparison with pure  $\text{AuNPs@ZrO}_2$ ,  $\text{PdNPs@ZrO}_2$ , and Au–Pd alloy NPs without the  $\text{ZrO}_2$  support in an aqueous suspension.

**Table 1.** Performance of Au–Pd Alloy NPs, AuNPs, and PdNPs for Cross-Coupling Reactions under Visible Light Irradiation (red numbers) and in the Dark (black numbers)

Reactions		Product Yield (%) <sup>[a]</sup>			TOF (h <sup>-1</sup> ) <sup>[b]</sup>		
		Au	Au–Pd	Pd	Au	Au–Pd	Pd
<b>1. Sonogashira coupling</b>		Light	0	80	90	0	4.7
		Dark	0	10	80	0	0.6
<b>2. Stille coupling</b>		Light	0	81	60	0	4.8
		Dark	0	33	47	0	1.9
<b>3. Hiyama coupling</b>		Light	0	71	55	0	4.2
		Dark	0	7	5	0	0.4
<b>4. Buchwald–Hartwig coupling</b>		Light	17	50	35	0.9	3.0
		Dark	15	30	0	0.8	1.8
<b>5. Ullmann coupling</b>		Light	0	35	16	0	2.1
		Dark	0	7	10	0	0.4

<sup>a</sup>The yields were calculated from the product content and the aryl iodide conversions measured by gas chromatography (GC). A Nelson halogen lamp (wavelengths of 400–750 nm) was used as the visible light source, and the light intensity was measured to be 0.45 W/cm<sup>2</sup>. The reaction was conducted at 45 ± 2 °C for 24 h. For the detailed reaction conditions, see the Experimental Section. <sup>b</sup>TOF (turnover frequency) values were calculated on the basis of the amount of Pd metal.

attributed to scattering. Because the distances between the alloy NPs on the ZrO<sub>2</sub> support are much smaller than those between the alloy NPs in their colloid suspension, the light scattering is much stronger for the supported alloy NPs than that for the unsupported NPs.<sup>24</sup> The light scattering is generally more significant at longer wavelengths (<600 nm).

**2.2. Photocatalytic Reactions.** 3-Iodotoluene was used as the aryl halide substrate to react with various coupling partners using Au–Pd alloy NPs under visible light irradiation (Table 1). The reactions were also conducted in the dark but with other conditions identical. For example, the temperature of the reaction mixture in the dark was kept the same as that of the reaction mixture under light (45 °C) by a water bath. The data in Table 1 show the results of visible light-enhanced cross-coupling reactions using the Au–Pd alloy NP catalyst.

It is evident that irradiation increased the extents of conversion of all the cross-coupling reactions (compared with the same reactions conducted in the dark). Control experiments using the support ZrO<sub>2</sub> (without Au–Pd alloy NPs) as the catalyst were performed. No conversion was observed for the reaction when the system was illuminated with light or when the reaction was conducted in the dark because ZrO<sub>2</sub> has a large band gap (5 eV) and exhibits negligible light absorption in the visible range.<sup>25</sup> Undoubtedly, the catalytic activity is due to the Au–Pd alloy NPs, and the catalytic enhancement observed when the system was irradiated is due to the alloy NPs.

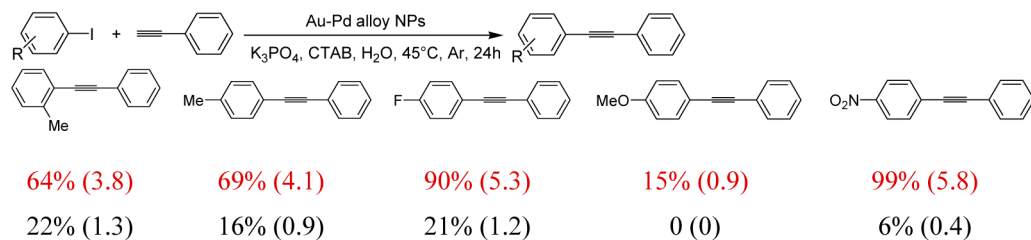
There have been many reports of cross-coupling reactions catalyzed via homogeneous or heterogeneous processes, but most of them need to be conducted at elevated temperatures (≥100 °C), even under reflux conditions.<sup>26–30</sup> This study

shows that visible light irradiation can drive the same reactions on the Au–Pd alloy NPs under much milder reaction conditions (45 °C), achieving very good yields, and no additional additives such as cocatalysts or phosphine ligands are required. The photocatalytic process at low reaction temperatures proposed in this study is thermodynamically preferred. Thus, utilizing light energy to promote the efficiency of this process is a green approach due to its lower energy input.

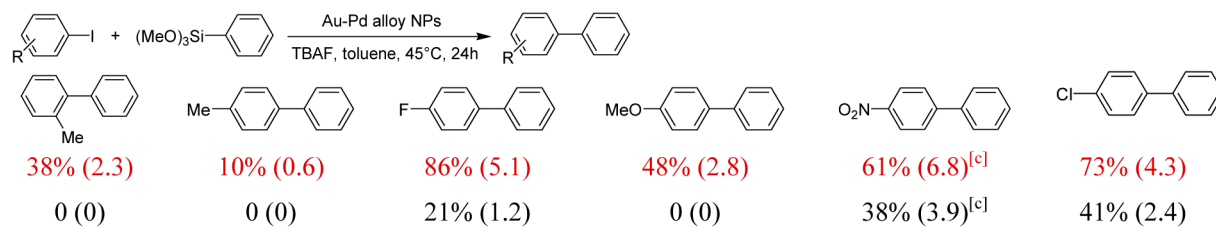
As shown in Table 1, for all the reactions PdNP catalysts exhibited better activity under irradiation than in the dark. The absorption of visible light and UV light by PdNPs can excite the electron interband transition,<sup>31</sup> and these excited electrons at the surface of the PdNPs enhance the catalytic ability of the PdNPs. AuNPs exhibit no catalytic activity for these reactions, whether under light irradiation or in the dark, except for the Buchwald–Hartwig reaction (17% under light, 15% in the dark). The Au–Pd alloy NPs exhibited superior catalytic activity when irradiated; the calculated TOF values for Au–Pd alloy NPs are much higher than those of pure AuNPs or PdNPs (approximately 1.7–4.2-fold) under light irradiation. This can be attributed to the fact that the charge heterogeneity of the alloy NP surface is greater than those of AuNP and PdNP surfaces,<sup>19</sup> which leads to a stronger interaction between the alloy NPs and reactant molecules.<sup>32,33</sup> The performance of the Au–Pd alloy NPs strongly depends on the Au/Pd ratio for the reactions in the presence and absence of light. It has been shown that when the Au/Pd molar ratio is 1/1.86, the surface charge heterogeneity is the greatest and results in optimal catalytic activity.<sup>19</sup>

Table 2. Au–Pd Alloy NPs Catalyzed Cross-Coupling Reactions with Different Aryl Halides under Visible Light Irradiation (red numbers) and in the Dark (black numbers)<sup>a</sup> [values in parentheses are the TOF values ( $\text{h}^{-1}$ )]<sup>b</sup>

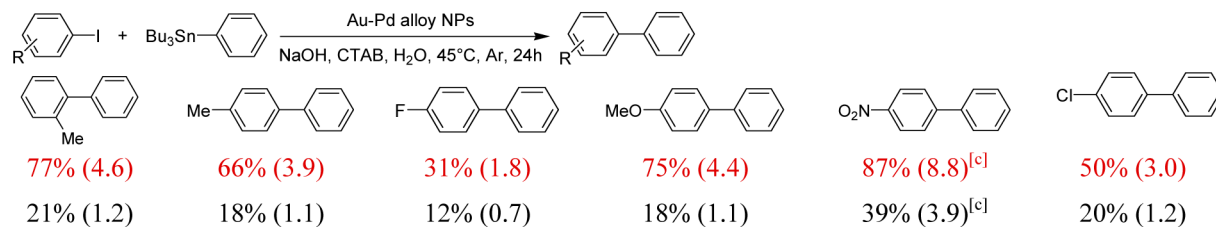
### 1. Sonogashira coupling



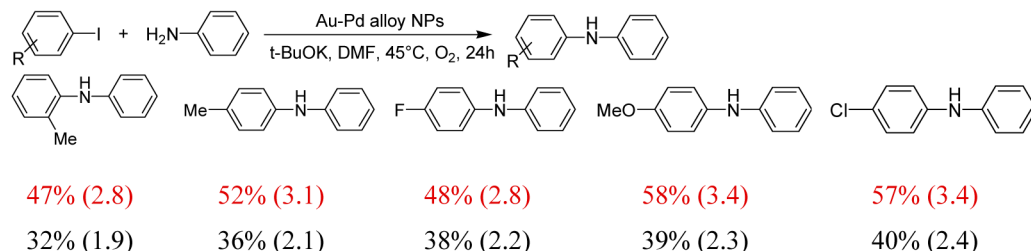
### 2. Hiyama coupling



### 3. Stille coupling



### 4. Buchwald–Hartwig coupling



<sup>a</sup>The yields were calculated from the product content and the aryl halide conversions measured by GC. The products were analyzed by GC and mass spectrometry. For detailed reaction conditions, see the Experimental Section. <sup>b</sup>TOF values were calculated on the basis of the amount of Pd metal.

<sup>c</sup>Reaction time of 14 h.

It is known that AuNPs exhibit strong visible light absorption due to the LSPR effect.<sup>34,35</sup> LSPR is the resonant light-induced coherent oscillation of charges at the metal–dielectric interface, established when the frequency of the incident light matches the frequency of metal surface electrons oscillating against the restoring force of their positive nuclei. Therefore, in addition to creating a NP surface with greater surface charge heterogeneity, gold in the Au–Pd alloy NPs enhances the ability of the NP to harvest the light energy [compared with that of PdNPs (see Figure 2)]. When the alloy NPs are irradiated with light, the conduction electrons gain the energy of the incident light, yielding Pd sites with light-excited electrons at the alloy NP surface. Hence, the intrinsic catalytic activity of the Pd sites is significantly enhanced at low reaction temperatures.

The general applicability of the Au–Pd alloy NP-photo-catalyzed cross-coupling reaction was investigated with a series of differently substituted aryl halides. As shown in Table 2, the light irradiation remarkably promoted the reaction in each case. High selectivities for the desired cross-coupling products were achieved regardless of whether the substituents were electron donors or acceptors. Thus, the visible light photocatalytic process using Au–Pd alloy NPs can drive various cross-coupling reactions with a broad range of substrates.

It is well-known that activation of C–Br and C–Cl bonds is much more difficult than activation of the C–I bond and in general requires harsher reaction conditions in the heterogeneous catalysis system.<sup>36</sup> In this study, we examined the catalytic activity of Au–Pd alloy NPs for reactions using

**Table 3.** Examples of Bromobenzene and Chlorobenzene as Substrates for Cross-Coupling Reactions Using Au–Pd Alloy NPs under Visible Light and UV Light Irradiation

Entry	Substrates	Product	Yield (%) <sup>[a]</sup>		TOF (h <sup>-1</sup> ) <sup>[c]</sup>	
			Visible light	UV light <sup>[b]</sup>	Visible light	UV light <sup>[b]</sup>
1	<chem>c1ccccc1Br</chem> + <chem>Bu3Sn-c1ccccc1</chem>	<chem>c1ccccc1-c2ccccc2</chem>	30 (18)	36	1.8 (1.1)	2.1
2	<chem>c1ccccc1Br</chem> + <chem>(MeO)3Si-c1ccccc1</chem>	<chem>c1ccccc1-c2ccccc2</chem>	23 (10)	31	1.4 (0.6)	1.8
3	<chem>c1ccccc1Br</chem> + <chem>H2N-c1ccccc1</chem>	<chem>c1ccccc1-N(c1ccccc1)C</chem>	28 (10)	40	1.7 (0.6)	2.4
4	<chem>c1ccccc1Cl</chem> + <chem>Bu3Sn-c1ccccc1</chem>	<chem>c1ccccc1-c2ccccc2</chem>	0 (0)	12	0	0.7
5	<chem>c1ccccc1Cl</chem> + <chem>(MeO)3Si-c1ccccc1</chem>	<chem>c1ccccc1-c2ccccc2</chem>	0 (0)	10	0	0.6

<sup>a</sup>The yields were calculated from the product content and the aryl halide conversions measured by GC. The values in parentheses are the data for reactions controlled under the same conditions in the dark. Reaction temperature of 65 °C. <sup>b</sup>The UV light reaction was conducted under UV lamp (UVP Blak-Ray B100AP High Intensity UV Lamp, 100 W, 365 nm UV) irradiation with a light intensity of 0.9 W/cm<sup>2</sup>, and the other reaction conditions were kept the same. <sup>c</sup>TOF values were calculated on the basis of the amount of Pd metal.

bromobenzene and chlorobenzene as substrates with light irradiation. Visible light can activate bromobenzene effectively, but the yields are much lower than those using iodobenzene (Table 3, entries 1–3). Surprisingly, we found that ultraviolet (UV) irradiation with higher intensity and energy could not only substantially improve the yields of the reactions (Table 2, entries 1–3) but also activate the reactions with chlorobenzenes that can hardly be activated under visible light irradiation (Table 3, entries 4 and 5). These results indicate that one can improve the catalytic activities by increasing light intensity and using shorter wavelength light.

**2.3. Impact of Light Intensity and Wavelength.** We investigated the dependence of catalytic activity on light intensity, and the results of the representative examples of Sonogashira, Hiyama, and Stille reactions are depicted in Figure 3. When the irradiation intensity was increased from 0.1 to 0.2, 0.3, 0.4, and 0.5 W/cm<sup>2</sup> with other reaction conditions unchanged, the extent of conversion of the reactions on the Au–Pd alloy NPs increased. There is a positive relationship between the intensity and reaction rate.

As shown in Figure 3, the results clearly exhibit an almost linear dependence. The contributions of light irradiation to the conversion efficiency were calculated by subtracting the extent of conversion of the reaction in the dark from the overall extent of conversion observed when the system was irradiated, with both reactions occurring at an identical reaction temperature. Here the conversion of the reaction in the dark is regarded as the contribution of the thermal effect. The relative contributions of light and thermal processes to the conversion efficiencies are shown in Figure 3. We can see that the higher the light intensity, the greater the contribution of irradiation to the overall conversion rate. When the light intensity is 0.1 W/cm<sup>2</sup>, the light contributions for these reactions were only 47% (Sonogashira), 20% (Hiyama), and 14% (Stille), and when the light intensity increased to 0.5 W/cm<sup>2</sup>, 90, 89, and 63%, respectively, of the conversion are due to irradiation. A stronger light intensity will induce a larger population of electrons at higher energy levels and create a stronger electromagnetic field around the NPs (surface enhancement effect), as reported for

AuNPs.<sup>37</sup> The transfer of the light-excited electrons of a metal nanoparticle to molecules adsorbed on the nanoparticles is well-known.<sup>38,39</sup> Such transfer induces the reaction of the molecules. The surface enhancement effect also contributes to a stronger interaction between the NPs and reactant molecules, and thus enhanced catalytic activity of the coupling reactions.

A useful tool for determining whether an observed reaction occurs via a photoinduced process or a thermocatalytic process is the action spectrum, which should show one-to-one mapping between the wavelength-dependent photocatalytic rate and the light extinction spectrum.<sup>40,41</sup> In this study, the reaction rates of the photocatalytic cross-coupling reactions using Au–Pd alloy NPs at 40 ± 2 °C under irradiation with different wavelengths were determined. Five LED lamps with wavelengths of 400 ± 5, 470 ± 5, 530 ± 5, 590 ± 5, and 620 ± 5 nm were used, and the rates were converted to the apparent quantum efficiencies (AQEs). The AQE was calculated using the relationship AQE (%) = [(Y<sub>light</sub> – Y<sub>dark</sub>)/(the number of incident photons)] × 100, where Y<sub>light</sub> and Y<sub>dark</sub> are the amounts of products formed under light irradiation and dark conditions, respectively. The plot of AQE versus the respective wavelengths is the action spectrum of the reaction. The action spectra of Sonogashira and Stille reactions are shown in Figure 4 as representative examples. Each action spectrum in the figure is compared with the light absorption spectrum of the Au–Pd alloy NPs and the spectrum of AuNPs.

The action spectra exhibit a few interesting features. First, action spectra of the cross-coupling reactions do not follow the absorption spectrum of the Au–Pd alloy NPs@ZrO<sub>2</sub> catalyst, which includes a substantial contribution from scattering. It means that the scattering has little impact on the catalytic performance. Second, a correspondence is observed between the AQE of the Sonogashira reaction and the light absorption of AuNPs (Figure 4a), which show the characteristic LSPR absorption peak in the range between 500 and 550 nm.<sup>34,35</sup> The PdNPs exhibited a high catalytic activity for the Sonogashira reaction in the dark (Table 1), indicating that the PdNPs can readily activate reactants of this reaction. Given that alloying with Au results in a loss of most of the activity in

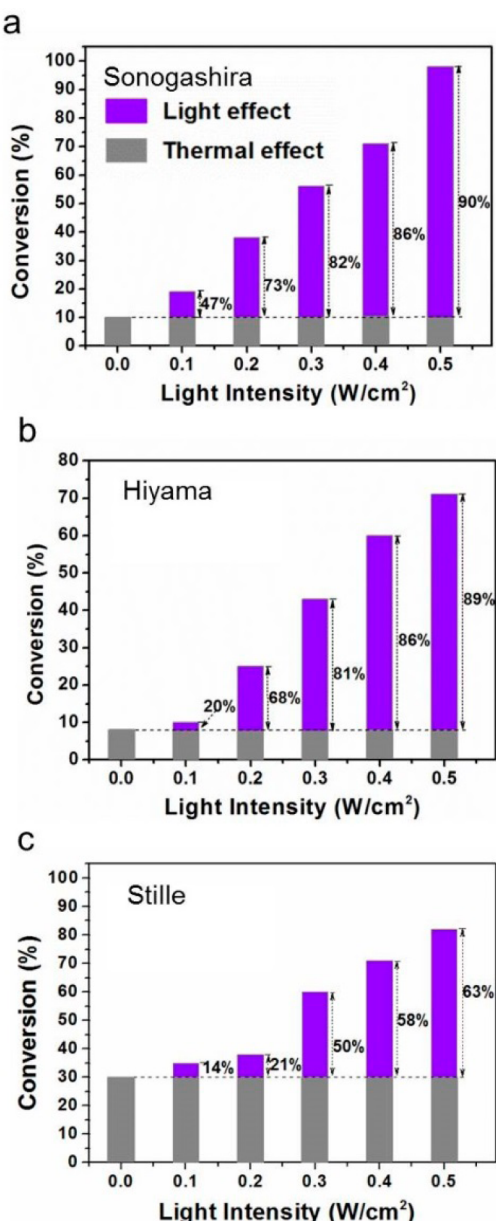


**Figure 3.** Dependence of the catalytic activity of Au–Pd alloy NPs for (a) Sonogashira, (b) Hiyama, and (c) Stille cross-coupling reactions on the intensity of light irradiation. The numbers with percentages show the contribution of the light irradiation effect. 3-Iodotoluene was used as the aryl halide substrate to react with the corresponding coupling partner under visible light irradiation. The reaction conversions were based on the average of two experiments. In the reactions for determining the light intensity dependence, a photometer was used to measure the light intensity; the other experimental conditions were kept the same. For the reaction conditions, see the Experimental Section.

the dark and AuNPs exhibited no activity for this reaction (Table 1), the reaction apparently takes place only at the Pd sites and is not affected by the higher surface charge heterogeneity of the alloy NPs. Thus, the function of gold in the alloy NP is apparently only to absorb the light energy. The light absorption of Au–Pd alloy NPs is obviously stronger than that of the pure PdNPs at all wavelengths (Figure 2). Gold nanostructures exhibit strong LSPR absorption of visible light, which can excite electrons to high energy levels. In the alloy

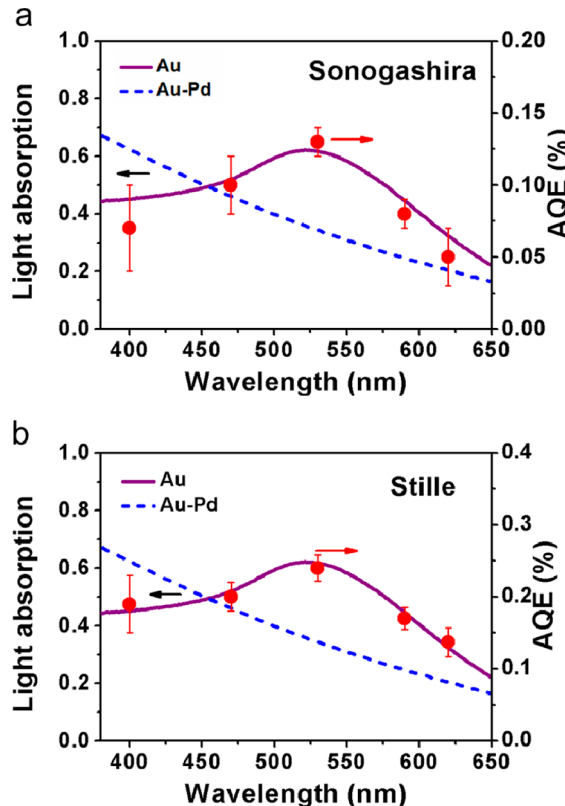


**Figure 4.** Action spectra for (a) Sonogashira and (b) Stille cross-coupling reactions. The light absorption spectra (left axis) are DR-UV-vis spectra of AuNPs (purple) and the Au–Pd alloy NPs (blue). 3-Iodotoluene was used as the aryl halide substrate to react with corresponding coupling partners under visible light irradiation. The AQE values were calculated on the basis of the average of three experiments. For details, see the Experimental Section.

NPs, these light-excited electrons can migrate to the surface Pd sites where they function like the light-excited electrons of the PdNPs, resulting in a significant enhancement of the catalytic performance of the alloy NPs. The action spectrum suggests that the enhancement of the catalytic performance is mainly due to the LSPR absorption of gold in the alloy NPs. The situation of the Stille reaction is similar to that of the Sonogashira reaction (Table 1); the action spectrum of the Stille reaction likewise follows the absorption spectrum of AuNPs (Figure 4b). Here, we can confirm that it is the Au that acts as an antenna that harvests visible light enhancing the reaction yield in alloy NP-catalyzed reactions.

The dependence of photocatalytic activity on light intensity and wavelength indicates that electrons excited by light absorption are responsible for the observed photocatalytic activity.<sup>42</sup> Because the rate of the catalyzed reactions is expected to depend on the population of electrons with sufficient energy to initiate the reaction of the reactant molecules, one can increase the number of light-excited electrons by applying a high light intensity. The electron energy sufficient to initiate the reaction of the molecules on the metal NPs is dependent on the actual reaction in question. Tuning the irradiation wavelength can increase the number of light-excited electrons with sufficient energy to induce the reaction and may also assist us in understanding the mechanism of the reactions.

**2.4. Impact of Temperature.** Another important feature of the photocatalytic process on metal NP catalysts is that the

photocatalytic activity of the NPs can be increased by elevating the reaction temperature.<sup>43,44</sup> This feature is also observed from the alloy NP photocatalysts in this study. For example, the extent of conversion of the Sonogashira reaction at 30 °C was only 11%, whereas the extent of conversion reached 100% when the temperature was increased to 60 °C in the same time interval (Figure 5a, blue dots). At a higher temperature, more

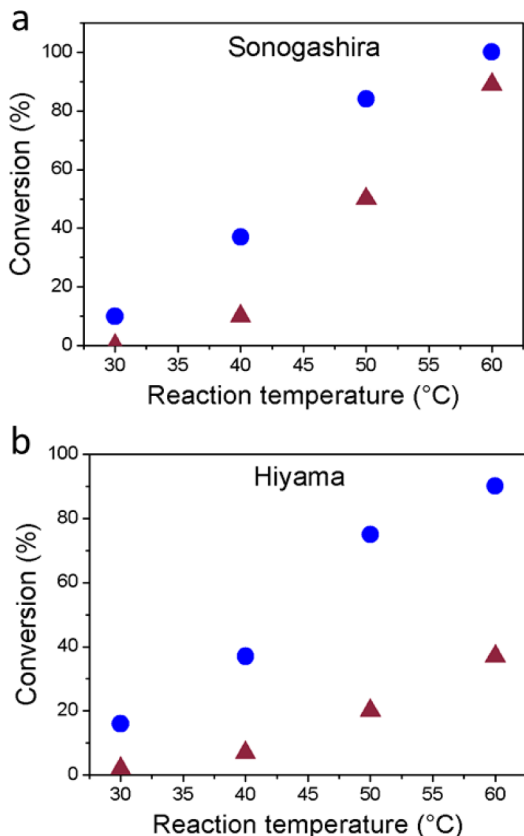


**Figure 5.** Dependence of catalytic activity on different reaction temperatures for (a) Sonogashira and (b) Hiyama reaction under a thermal heating process in the dark (triangles) and the light irradiation process (circles). 3-Iodotoluene was used as the aryl halide substrate to react with corresponding coupling partners under light irradiation and in the dark. The light intensity was 0.45 W/cm<sup>2</sup>.

electrons of the metal NPs populate higher energy levels, but these electrons can still gain energy from the incident light. Thus, upon irradiation, the number of electrons with sufficient energy to initiate the reaction of the molecules adsorbed on the metal NPs is greater. At a low reaction temperature, the photoexcitation contributes dominantly to the photocatalytic activity and the photothermal effect would contribute much less.<sup>20</sup> For many catalyzed reactions involving the interaction between light-excited electrons of a catalyst with reactant molecules, high reaction temperatures are not a prerequisite to drive them. Light irradiation can yield excited electrons with sufficient energy at low reaction temperatures and facilitate the reactions of the reactants. The metal NPs have the capacity to couple the stimuli of light irradiation and heat to drive the catalytic reaction.<sup>43</sup> This property not only distinguishes them from semiconductor photocatalysts but also reveals the potential of the NPs to utilize the infrared radiation in sunlight, which accounts for a large fraction of the solar spectrum and could be used to heat the NPs, further facilitating the reaction.

Because the photocatalytic activity of the alloy NP photocatalysts varies with temperature, the apparent activation energies of Sonogashira and Hiyama reactions were estimated by using the Arrhenius equation and kinetic data for photocatalytic reactions conducted over the range of 30–60 °C. As shown in Figure 6, the difference between the activation

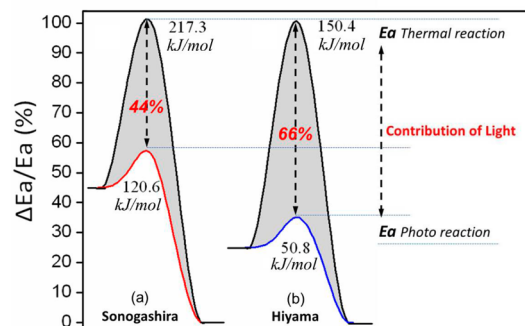


**Figure 6.** Apparent activation energies of (a) Sonogashira and (b) Hiyama reactions calculated for the photoreaction and the reaction in the dark. The contribution of light irradiation is calculated from the difference in the extents of conversion of two processes (with and without light) and presented as a percentage (Y axis). 3-Iodotoluene was used as the aryl halide substrate to react with corresponding coupling partners under light irradiation and in the dark. The light intensity was 0.45 W/cm<sup>2</sup>.

energies of the light-enhanced process and the process in the dark ( $\Delta E_a$ ) indicates the reduction in the measured activation energy due to irradiation. For example, the estimated activation energy is ~217 kJ/mol for the Sonogashira reaction in the dark (Figure 6a), while it is ~120 kJ/mol for the photocatalytic reaction under visible light irradiation. Thus, light irradiation can reduce the activation energy of the Sonogashira reaction by 97 kJ/mol, which represents 44% of the “uncatalyzed” activation energy. Similarly, the activation energy of the Hiyama reaction was reduced by 66% (Figure 6b). The fact that irradiation substantially reduces the activation energy demands that the photocatalytic process have a mechanism different from that of the process in the dark.

**2.5. Proposed Mechanism.** The cross-coupling reactions involve two essential steps: breaking the carbon–iodine bond in aryl iodide and activation of the coupling partner molecules that then facilitates transmetalation.<sup>45,46</sup> It has been postulated that the transfer of an electron from the Pd atoms to the halogen atoms is involved in facilitating carbon–halogen bond cleavage in the Pd heterocatalysis.<sup>20</sup> This is effectively the heteroanalogue of the familiar homogeneous oxidative addition step involving ligated Pd(0). In this study, when the PdNPs were irradiated with light, enhanced catalytic performance was observed. Because the absorption of light by PdNPs excites the electrons of the PdNPs to the high-energy band, it is deduced that the light-excited electrons at the surface of the PdNPs can enhance the catalytic ability. Given that AuNPs exhibit no catalytic activity for most of the reactions, it is reasonable to believe that the light-excited electrons at the surface Pd sites of the alloy NPs facilitate the reactions. The linear dependence of the photoinduced reaction rate on the light intensity, observed in Figure 3, usually suggests an electron-driven chemical process on the metal surface.<sup>42</sup> Also, transient electron transfer from a light-excited metal NP to a chemically adsorbed molecule is well-known.<sup>38,39</sup> Electrons of alloy NPs are excited

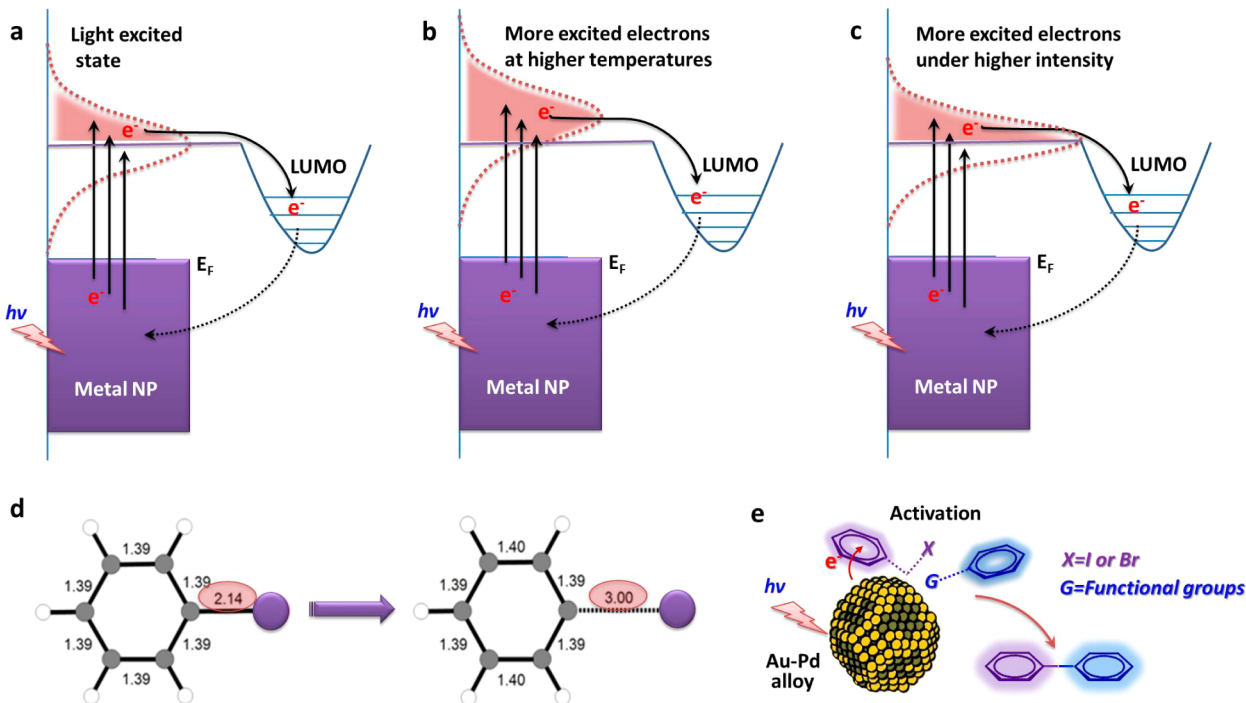


**Figure 7.** Proposed mechanism for the photocatalytic cross-coupling reactions. (a) Light irradiation excites electrons of an alloy NP to high energy levels, and the transfer of the excited electrons with sufficient energy from the alloy NP to the LUMO of molecules adsorbed on the NP can take place, activating the reaction. The electrons finally return to the metal NP at a lower energy.<sup>38</sup> (b) At higher reaction temperatures, more excited electrons populate higher energy levels of the metal NPs, which can be readily transferred to the LUMO of the absorbed molecule. (c) Under a higher irradiation intensity, more electrons of the metal NPs populate higher energy levels, resulting in more electron transfers to the LUMO of the absorbed molecule and higher reaction rates. (d) DFT calculations on the reactant iodobenzene before (left) and after (right) the transfer of one electron from the NP surface to the reactant molecule. The C—I bond is elongated because of the electron transfer, which facilitates the activation of reactions. (e) Schematic diagram of the pathway for the photocatalytic cross-coupling reactions.

by light irradiation; the excited electrons transfer from the alloy NP surface to the LUMO of a molecule adsorbed on the NP, activating the substrate. The electron can finally return to the metal at a lower energy (Figure 7a–c). We therefore performed DFT calculations on the transfer of one electron from the NP surface to the reactant iodobenzene molecule. The simulation suggests that when one electron enters an unoccupied orbital, the C—I bond will become longer (from 0.214 to 0.300 nm), so the cleavage of the C—I bond will be much easier (Figure 7d). For the reactions in which the rate-determining step is C—I bond cleavage, irradiation will facilitate the transfer of an electron from the NP to the adsorbed aryl iodide molecule, yielding a transient negative ion species. Loss of iodide ion will afford either an adsorbed phenyl radical or a true organometallic aryl–palladium iodide complex on the surface and then activate the reactions (Figure 7e).

Given that the PdNPs exhibited catalytic activity for most of the reactions in the dark, it is believed that activating iodobenzene molecules on the surface Pd sites is not difficult. The fact that the Buchwald–Hartwig coupling reaction on PdNPs did not occur in the dark suggests that the surface Pd sites cannot activate aniline in the dark. The significant catalytic activity of PdNPs for this reaction under light should be due to the activation of aniline on the PdNP surface under irradiation. Aniline has a strong interaction with AuNP surfaces and is often used for the surface-enhanced Raman spectral study,<sup>34</sup> and this explains the observed catalytic activity of the AuNPs in the dark. The fact that the Au–Pd alloy NPs exhibited catalytic activity superior to that of both the AuNPs and the PdNPs in

the dark indicates that the charge heterogeneity of the alloy NP surface also enhances the catalytic activity.

The heterogeneous catalytic processes of the coupling reactions examined in this study have multiple steps and are by no means well-understood.<sup>47,48</sup> In this regard, we focused only on possible roles for the light-excited electrons afforded at the NP surfaces by irradiation. The delineation of subsequent steps is a profound challenge but is beyond the scope of this preliminary survey.

### 3. CONCLUSIONS

The findings in this study demonstrate that irradiation of Au–Pd alloy NPs can significantly enhance the intrinsic catalytic activity of Pd at lower temperatures for a number of Pd-catalyzed cross-coupling reactions. An outstanding feature of the Au–Pd alloy NPs is their ability to efficiently concentrate the energy of a photon flux to a very small volume and to transfer this energy to the adsorbed molecules to induce their reaction on the surface. These catalytic cross-coupling processes are due to the interaction of light-excited electrons of the catalyst with the reactant molecules, while high temperatures are not a prerequisite for driving them. The reaction rate depends on the number of light-excited electrons and the number of reactant molecules on the catalyst surface. The number of reactant molecules on the surface depends mainly on the affinity of the surface for the reactants. Pd sites have a strong affinity for many organic molecules. The number of light-excited electrons can be increased by applying a high light intensity. Although we focused on Au–Pd nanostructures,

the discussed mechanisms may be universal, and similar principles could be used in the design of various photocatalysts comprising any of a range of plasmonic metals and a catalytically active transition metal.<sup>37</sup> Thus, we have been able to utilize a low-energy and -density source to drive a wide range of useful chemical transformations. In these reaction systems, the energy efficiency is high, because of the specific absorption of the light only by the NP catalysts, and not by the solvent, the oxide support, the atmosphere, or the reaction vessel. The findings reported here reveal the possibility of green cross-coupling reactions driven by visible light at temperatures slightly above room temperature.

#### 4. EXPERIMENTAL SECTION

**4.1. Chemicals.** Zirconium(IV) oxide ( $\text{ZrO}_2$ , <100 nm particle size, TEM), gold(III) chloride trihydrate ( $\text{HAuCl}_4 \cdot 3\text{H}_2\text{O}$ , ≥99.9% trace metal basis), palladium(II) chloride ( $\text{PdCl}_2$ , ReagentPlus, 99%), sodium borohydride, powder ( $\text{NaBH}_4$ , ≥98.0%), hydrochloric acid [HCl, 32% (w/w), analytical reagent, Chem-Supply], and *N,N*-dimethylformamide (DMF, anhydrous, 99.8%, total impurities, <0.005% water) were purchased from Sigma-Aldrich (unless otherwise noted) and used as received without further purification. The water used in all experiments was prepared by being passed through an ultrapurification system.

**4.2. Preparation of Catalysts.** Au–Pd alloy NPs (1.5 wt % Au–1.5 wt % Pd supported on  $\text{ZrO}_2$ , Au/Pd molar ratio of 1/1.86) were prepared by the impregnation–reduction method.  $\text{ZrO}_2$  powder (2.0 g) was dispersed into a  $\text{HAuCl}_4$  (15.2 mL, 0.01 M) and  $\text{PdCl}_2$  (28.3 mL, 0.01 M) aqueous solution under magnetic stirring at room temperature. A lysine (16 mL, 0.53 M) aqueous solution was then added to the mixture while it was vigorously stirred for 30 min, and the pH value was determined to be 8–9. To this suspension was added dropwise a freshly prepared aqueous  $\text{NaBH}_4$  (3 mL, 0.35 M) solution in 20 min, followed by an addition of an HCl (3 mL, 0.3 M) solution. The mixture was aged for 24 h, and then the solid was separated by centrifugation, washed with water (three times) and ethanol (once), and dried at 60 °C in a vacuum oven for 24 h. The dried powder was used directly as a catalyst. Pure Au NPs (3 wt %) and Pd NPs (3 wt %) were prepared via a similar method but using different quantities of  $\text{HAuCl}_4$  and  $\text{PdCl}_2$  aqueous solutions.

**4.3. Characterization of Catalysts.** A transmission electron microscope (TEM) study and line profile analysis by an energy dispersion X-ray (EDX) spectrum technique of the photocatalysts were conducted on a Philips CM200 TEM with an accelerating voltage of 200 kV. Element line scanning was conducted on a Bruker energy dispersion X-ray (EDX) scanner attached to a JEOL-2200FS TEM with a scanning beam diameter of ≥1.0 nm. The Au and Pd contents of the prepared catalysts were determined by energy dispersion X-ray spectrum (EDS) technology using the attachment to a FEI Quanta 200 environmental scanning electron microscope (SEM). Diffuse reflectance UV-visible (DR-UV-vis) spectra of the sample powders were examined with a Varian Cary 5000 spectrometer with  $\text{BaSO}_4$  as a reference.

**4.4. Photocatalytic Reactions.** A 25 mL Pyrex round-bottom flask was used as the reaction container, and after the reactants and catalyst had been added, the flask was sealed with a rubber septum cap. The flask was irradiated with magnetic stirring using a halogen lamp (from Nelson, wavelength in the range of 400–750 nm) as the visible light source, and the light

intensity was measured to be 0.45 W/cm<sup>2</sup>. The temperature of the reaction system was carefully controlled with an air conditioner attached to the reaction chamber. The reaction system under light illumination was maintained at the same temperature as the corresponding reaction system in the dark to ensure that the comparison is meaningful. All the reactions in the dark were conducted using a water bath placed above a magnetic stirrer to control the reaction temperature; the reaction flask was wrapped with aluminum foil to avoid exposure of the reaction mixture to light. At given irradiation time intervals, 2 mL aliquots were collected and then filtered through a Millipore filter (pore size of 0.45 μm) to remove the catalyst particulates. The liquid-phase products were analyzed with an Agilent 6890 gas chromatography (GC) HP-5 column to measure the change in the concentrations of reactants and products. An Agilent HP5973 mass spectrometer was used to identify the product. For the reactions using  $\text{H}_2\text{O}$  as the solvent, the product was extracted with dichloromethane ( $\text{CH}_2\text{Cl}_2$ ) before GC analysis. The GC conversions and selectivities were calculated from the product content and the aryl halide conversions.

**4.4.1. Sonogashira Cross-Coupling Reactions.** Aryl iodide (1 mmol), alkyl alkyne (1.2 mmol), photocatalysts (50 mg), cetyltrimethylammonium bromide (CTAB) (1 mmol), and  $\text{K}_3\text{PO}_4$  (2 mmol) were added to 10 mL of  $\text{H}_2\text{O}$ . The reaction temperature was 45 ± 2 °C, under a 1 atm argon atmosphere, with a reaction time of 24 h.

**4.4.2. Hiyama Cross-Coupling Reactions.** Aryl iodide (1 mmol), trimethoxyphenylsilane (1.5 mmol), photocatalysts (50 mg), and tetrabutylammonium fluoride (TBAF) (1.2 mmol) were added to 5 mL of toluene. The reaction temperature was 45 ± 2 °C, with a reaction time of 24 h.

**4.4.3. Stille Cross-Coupling Reactions.** Aryl iodide (1 mmol), tributylphenylstannane (1.2 mmol), photocatalysts (50 mg), cetyltrimethylammonium bromide (CTAB) (1 mmol), and NaOH (3 mmol) were added to 10 mL of  $\text{H}_2\text{O}$ . The reaction temperature was 45 ± 2 °C, under a 1 atm argon atmosphere, with a reaction time of 24 h.

**4.4.4. Ullmann Cross-Coupling Reactions.** Aryl iodide (1 mmol), photocatalysts (50 mg), and NaOH (3 mmol) were added to 10 mL of an EtOH/ $\text{H}_2\text{O}$  mixture [1/1 (v/v)]. The reaction temperature was 45 ± 2 °C, with a reaction time of 24 h.

**4.4.5. Buchwald–Hartwig Cross-Coupling Reactions.** Aryl iodide (1 mmol), aniline (1.2 mmol), photocatalysts (50 mg), and potassium *tert*-butoxide (*t*-BuOK) (3 mmol) were added to 10 mL of *N,N*-dimethylformamide (DMF). The reaction temperature was 45 ± 2 °C, with a reaction time of 24 h.

**4.4.6. Action Spectrum Experiments.** LED lamps (Tongyifang, Shenzhen, China) with wavelengths of 400 ± 5 nm (TYF-H030 G45), 470 ± 5 nm (TYF-H030 G35), 530 ± 5 nm (TYF-H030 G35), 590 ± 5 nm (TYF-H030 G38), and 620 ± 5 nm (TYF-H030 G32) were used as the light source. The light intensity was measured to be 0.50 W/cm<sup>2</sup>, and the other reaction conditions were identical to those of typical reaction procedures.

**4.5. DFT Calculation.** The geometries of all the species were optimized at the level of DFT with Becke's<sup>49</sup> three-parameter exchange and Lee–Yang–Parr correlation functional<sup>50</sup> implemented in Orca.<sup>51</sup> Ahlrichs' triple- $\zeta$  valence basis set<sup>52</sup> TZVP was employed to describe the orbitals of all atoms involved. The iodobenzene molecule and its corresponding

negative ion were fully optimized as defined by the B3LYP/TZVP method.

## AUTHOR INFORMATION

### Corresponding Author

\*E-mail: hy.zhu@qut.edu.au.

### Notes

The authors declare no competing financial interest.

## ACKNOWLEDGMENTS

The authors gratefully acknowledge financial support from the Australia Research Council (ARC DP110104990).

## REFERENCES

- (1) De Mejere, A.; Diederich, F. *Metal-Catalysed Cross-Coupling Reactions*, 2nd ed.; Wiley-VCH: Weinheim, Germany, 2004.
- (2) Nicolaou, K. C.; Bulger, P. G.; Sarlah, D. *Angew. Chem., Int. Ed.* **2005**, *44*, 4442–4489.
- (3) Johansson-Seechurn, C. C. C.; Kitching, M. O.; Colacot, T. J.; Snieckus, V. *Angew. Chem., Int. Ed.* **2012**, *51*, 5062–5085.
- (4) Buchwald, S. L. *Acc. Chem. Res.* **2008**, *41*, 1439–1439.
- (5) Magano, J.; Dunetz, J. R. *Chem. Rev.* **2011**, *111*, 2177–2250.
- (6) Balanta, A.; Godard, C.; Claver, C. *Chem. Soc. Rev.* **2011**, *40*, 4973–4985.
- (7) Molnar, A. *Chem. Rev.* **2011**, *111*, 2251–2320.
- (8) Campbell, C. T.; Parker, S. C.; Starr, D. E. *Science* **2002**, *298*, 811–814.
- (9) Lei, Y.; Mahmood, F.; Lee, S.; Greeley, J.; Lee, B.; Seifert, S.; Winans, R. E.; Elam, J. W.; Meyer, R. J.; Redfern, P. C.; Teschner, D.; Schlägl, R.; Pellin, M. J.; Curtiss, L. A.; Vajda, S. *Science* **2010**, *328*, 224–228.
- (10) Wittstock, A.; Zielasek, V.; Biener, J.; Friend, C. M.; Baumer, M. *Science* **2010**, *327*, 319–322.
- (11) Lu, C. L.; Prasad, K. S.; Wu, H. L.; Ho, J. A. A.; Huang, M. H. *J. Am. Chem. Soc.* **2010**, *132*, 14546–14553.
- (12) Narayana, J. M. R.; Stephenson, C. R. *J. Chem. Soc. Rev.* **2011**, *40*, 102–113.
- (13) Pirnot, M. T.; Rankic, D. A.; Martin, D. B. C.; MacMillan, D. W. C. *Science* **2013**, *339*, 1593–1596.
- (14) Nagib, D. A.; MacMillan, D. W. C. *Nature* **2011**, *480*, 224–228.
- (15) Shih, H. W.; Vander Wal, M. N.; Grange, R. L.; MacMillan, D. W. C. *J. Am. Chem. Soc.* **2010**, *132*, 13600–13603.
- (16) Palmisano, G.; Augugliaro, V.; Pagliaro, M.; Palmisano, L. *Chem. Commun.* **2007**, *33*, 3425–3437.
- (17) Hoffmann, N. *Chem. Rev.* **2008**, *108*, 1052–1103.
- (18) Yoon, T. P.; Ischay, M. A.; Du, J. *Nat. Chem.* **2010**, *2*, 527–532.
- (19) Sarina, S.; Zhu, H.; Jaatinen, E.; Xiao, Q.; Liu, H.; Jia, J.; Chen, C.; Zhao, J. *J. Am. Chem. Soc.* **2013**, *135*, 5793–5801.
- (20) Wang, F.; Li, C.; Chen, H.; Jiang, R.; Sun, L. D.; Li, Q.; Wang, J.; Yu, J. C.; Yan, C. H. *J. Am. Chem. Soc.* **2013**, *135*, 5588–5601.
- (21) Huang, X.; Li, Y.; Chen, Y.; Zhou, H.; Duan, X.; Huang, Y. *Angew. Chem., Int. Ed.* **2013**, *52*, 6063–6067.
- (22) Lee, Y. W.; Kim, N. H.; Lee, K. Y.; Kwon, K.; Kim, M.; Han, S. W. *J. Phys. Chem. C* **2008**, *112*, 6717–6722.
- (23) Chen, Y. H.; Tseng, Y. H.; Yeh, C. S. *J. Mater. Chem.* **2002**, *12*, 1419–1422.
- (24) Prodan, E.; Radloff, C.; Halas, N. J.; Norlander, P. *Science* **2003**, *302*, 419–422.
- (25) Emeline, A.; Kataeva, G. V.; Rudakova, A. S.; Ryabchuk, V. K.; Serpone, N. *Langmuir* **1998**, *14*, 5011–5022.
- (26) For Sonogashira reactions, see: (a) Ciriminna, R.; Pandarus, V.; Gingras, G.; Béland, F.; Demma Carà, P.; Pagliaro, M. *ACS Sustainable Chem. Eng.* **2013**, *1*, 57–61. (b) Pandarus, V.; Gingras, G.; Béland, F.; Ciriminna, R.; Pagliaro, M. *Org. Process Res. Dev.* **2012**, *16*, 117–122. (c) Srinivas, K.; Srinivas, P.; Prathima, P. S.; Balaswamy, K.; Sridhar, B.; Rao, M. M. *Catal. Sci. Technol.* **2012**, *2*, 1180–1187. (d) Schweizer, S.; Becht, J. M.; Le Drian, C. *Adv. Synth. Catal.* **2007**, *349*, 1150–1158.
- (27) For Stille reactions, see: (a) Espinet, P.; Echavarren, A. M. *Angew. Chem., Int. Ed.* **2004**, *43*, 4704–4734. (b) DelPozo, J.; Carrasco, D.; Pérez-Temprano, M. H.; García-Melchor, M.; Álvarez, R.; Casares, J. A.; Espinet, P. *Angew. Chem., Int. Ed.* **2013**, *52*, 2189–2193.
- (28) For Hiyama reactions, see: (a) Diebold, C.; Derible, A.; Becht, J. M.; Le Drian, C. *Tetrahedron* **2012**, *69*, 264–267. (b) Zhang, L.; Li, P.; Li, H.; Wang, L. *Catal. Sci. Technol.* **2012**, *2*, 1859–1864.
- (29) For Buchwald–Hartwig reactions, see: (a) Paul, P.; Sengupta, P.; Bhattacharya, S. *J. Organomet. Chem.* **2013**, *724*, 281–288. (b) Liu, X.; Zhang, S. *Synlett* **2011**, *8*, 1137–1142. (c) Rout, L.; Jammi, S.; Punniyamurthy, T. *Org. Lett.* **2007**, *9*, 3397–3399. (d) Pan, K.; Ming, H.; Yu, H.; Huang, H.; Liu, Y.; Kang, Z. *Dalton Trans.* **2012**, *41*, 2564–2566. (e) Kidwai, M.; Mishra, N. K.; Bhardwaj, S.; Jahan, A.; Kumar, A.; Mozumdar, S. *ChemCatChem* **2010**, *2*, 1312–1317. (f) Jammi, S.; Sakthivel, S.; Rout, L.; Mukherjee, T.; Mandal, S.; Mitra, R.; Saha, P.; Punniyamurthy, T. *J. Org. Chem.* **2009**, *74*, 1971–1976.
- (30) For Ullmann reactions, see: (a) Layek, K.; Maheswaran, H.; Kantam, M. L. *Catal. Sci. Technol.* **2013**, *3*, 1147–1150. (b) Wang, L.; Lu, W. *Org. Lett.* **2009**, *11*, 1079–1082. (c) Gäddä, T. M.; Kawanishi, Y.; Miyazawa, A. *Synth. Commun.* **2012**, *42*, 1259–1267.
- (31) Fan, G.; Qu, S.; Wang, Q.; Zhao, C.; Zhang, L.; Li, Z. *J. Appl. Phys.* **2011**, *109*, 023102.
- (32) Chen, M. S.; Kumar, D.; Yi, C. W.; Goodman, D. W. *Science* **2005**, *310*, 291–293.
- (33) Tang, W. J.; Henkelman, G. *J. Chem. Phys.* **2009**, *130*, 194504.
- (34) Kamat, P. V. *J. Phys. Chem. B* **2002**, *106*, 7729–7744.
- (35) Mulvaney, P. *Langmuir* **1996**, *12*, 788–800.
- (36) Yin, L.; Liebscher, J. *Chem. Rev.* **2007**, *107*, 133–173.
- (37) Sarina, S.; Waclawik, E. R.; Zhu, H. *Green Chem.* **2013**, *15*, 1814–1833.
- (38) Brus, L. *Acc. Chem. Res.* **2008**, *41*, 1742–1749.
- (39) Lindstrom, C. D.; Zhu, X. Y. *Chem. Rev.* **2006**, *106*, 4281–4300.
- (40) Tanaka, A.; Sakaguchi, S.; Hashimoto, K.; Kominami, H. *ACS Catal.* **2013**, *3*, 79–85.
- (41) Kowalska, E.; Abea, R.; Ohtania, B. *Chem. Commun.* **2009**, *2*, 241–243.
- (42) Christopher, P.; Xin, H. L.; Linic, S. *Nat. Chem.* **2011**, *3*, 467–472.
- (43) Linic, S.; Christopher, P.; Ingram, D. B. *Nat. Mater.* **2011**, *10*, 911–921.
- (44) Christopher, P.; Xin, H. L.; Marimuthu, A.; Linic, S. *Nat. Mater.* **2012**, *11*, 1044–1050.
- (45) Xue, L. Q.; Lin, Z. Y. *Chem. Soc. Rev.* **2010**, *39*, 1692–1705.
- (46) Diederich, F.; Stang, P. *Metal-catalyzed Cross-coupling Reactions*; Wiley-VCH: Weinheim, Germany, 1998.
- (47) Phan, N. T. S.; Van Der Sluys, M.; Jones, C. W. *Adv. Synth. Catal.* **2006**, *348*, 609–679.
- (48) Fihri, A.; Bouhrara, M.; Nekoueishahraki, B.; Basset, J. M.; Polshettiwar, V. *Chem. Soc. Rev.* **2011**, *40*, 5181–5203.
- (49) Becke, A. D. *J. Chem. Phys.* **1993**, *98*, 5648.
- (50) Lee, C.; Yang, W.; Parr, R. G. *Phys. Rev. B* **1988**, *37*, 785–789.
- (51) Neese, F. *WIREs Computational Molecular Science* **2012**, *2*, 73–78.
- (52) Schaefer, A.; Huber, S.; Ahlrichs, R. *J. Chem. Phys.* **1994**, *100*, 5829–5835.